

I. Devic design and micro-nano fabrication

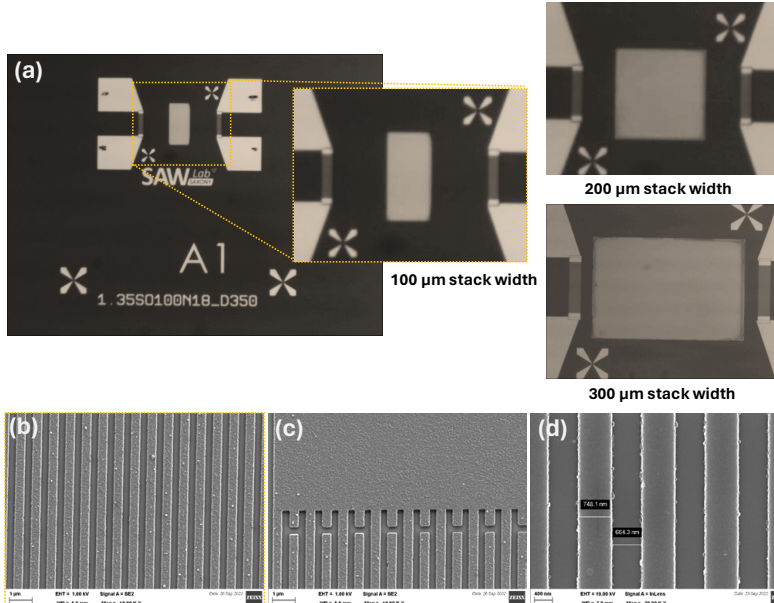


FIG 1. Optical images and scanning electron microscopy (SEM) images of fundamental-mode Surface Acoustic Wave (SAW) magnetoacoustic nonreciprocal low-loss RF isolator for efficient control of NV^- centers. (a) Optical image of SAW interdigital transducers and magnetic stacks with dimensions of $100 \mu\text{m} \times 300 \mu\text{m}$, $200 \mu\text{m} \times 300 \mu\text{m}$ and $300 \mu\text{m} \times 300 \mu\text{m}$. (b-d) scanning electron microscopy (SEM) images of IDTs.

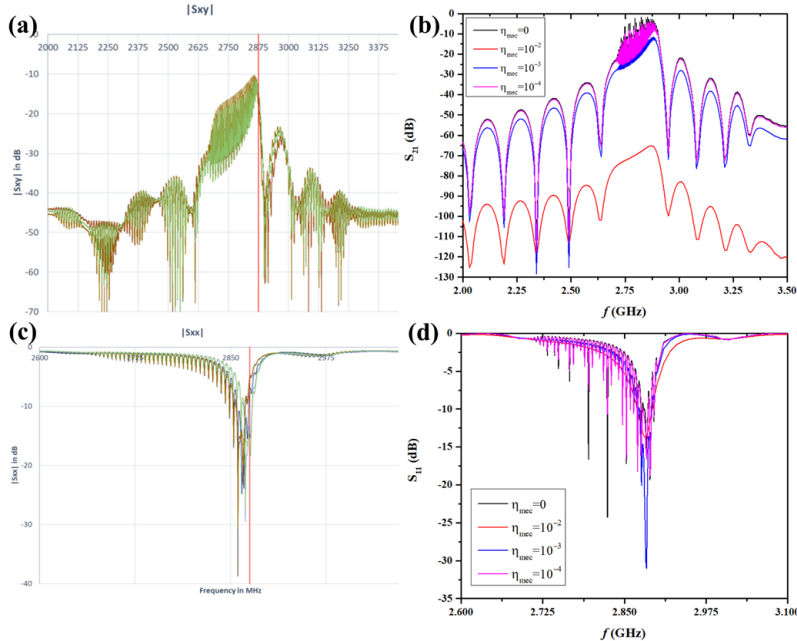


FIG 2. Simulation design and experimental measurement of the fabricated 2.87 GHz SAW delay line. (a) Experimental and (b) Simulated S_{xy} parameters. (c) Experimental and (d) Simulated S_{xx} parameters.

results in decreased S_{xy} magnitude and diminished modulation of the SAW resonance peak ("triple transit echo") caused by reflections between the IDTs near fundamental mode. The presence of triple transit echo confirms the strong magnitude and long propagation distance of fundamental SAW mode, which holds promise for the efficient excitation of strong spin wave for the coherent control of NV^- centers.

The optical image and scanning electron microscopy (SEM) images of fundamental-mode Surface Acoustic Wave (SAW) magnetoacoustic nonreciprocal low-loss RF isolator for efficient control of NV^- centers are shown in Figure 1. The transmission and receiving IDT Al electrodes with a fundamental mode of ~ 2.87 GHz were patterned on bulk LiNbO₃ substrate via laser lithography, e-beam lithography, e-beam metal evaporation and lift-off technique. The magnetic stacks FeGaB (20nm) /SiO₂(5nm)/ FeGaB (20nm) with dimensions of $100 \mu\text{m} \times 300 \mu\text{m}$, $200 \mu\text{m} \times 300 \mu\text{m}$ and $300 \mu\text{m} \times 300 \mu\text{m}$ were deposited by magnetron sputtering with 200 Oe bias field 45 degrees with respect to the SAW propagation direction. A 1:1 2D finite element model was built in COMSOL Multiphysics to design the SAW delay lines. The electrostatic module was combined with solid mechanics module to simulate piezoelectrically induced Rayleigh wave excited by SAW delay line under different mechanical and dielectric damping. The S parameters were experimentally measured by RF probes connected to a vector network analyzer. The fabricated SAW delay line shows a low insertion loss of ~ 10 dB at 2.87 GHz, which is excellent to control the ground states of NV^- centers, as shown in Figure 2 (a). The simulated S parameters agree well with probe measurement, suggesting the effectiveness of the FEM model in designing the IDTs, as shown in Figure 2(b). The increased mechanical damping

II. Strong magnetoacoustic absorption and non-reciprocity

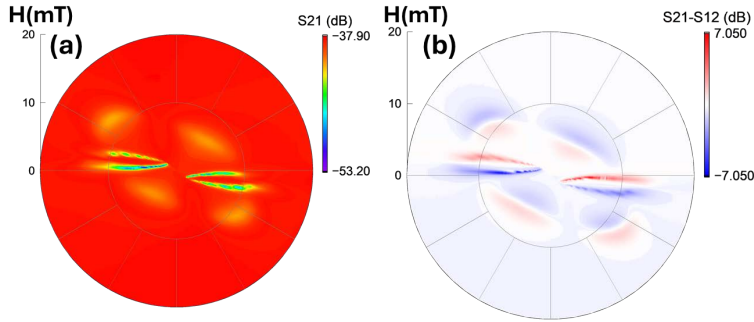


FIG 3. Strong magnetoacoustic absorption and non-reciprocity of the fundamental-mode Surface Acoustic Wave (SAW) magnetoacoustic nonreciprocal low-loss RF isolator with a magnetic stack dimension of $300\ \mu\text{m}\times 300\ \mu\text{m}$. (a) S_{21} as a function of rotating bias magnetic field. A strong absorption of 15.3 dB was observed at -150 degrees and 0 degrees. (b) Non-reciprocity evaluated by $S_{21}-S_{12}$. A strong non-reciprocity of 23.5 dB/mm was observed.

The S parameters as a function of rotating magnetic field were measured to characterize the absorption and non-reciprocity owing to the strong coupling between the non-reciprocal spin waves and the fundamental mode surface acoustic wave. Under a rotating bias magnetic field, fundamental-mode Surface Acoustic Wave (SAW) magnetoacoustic nonreciprocal low-loss RF isolator with $300\times 300\ \mu\text{m}^2$ non-reciprocal magnetic stack shows a magnetic absorption of 15.25 dB and a strong transmission non-reciprocity of 7.05 dB at 2.8 GHz, leading to giant non-reciprocity of 23.5 dB/mm per magnetic length, as shown in Figure 3. This value is slightly higher than 22 dB/mm demonstrated in the previous device with 1425 MHz 5th order mode [11-12]. Note that the device has a maximum transmission of ~ 30 dB, which is 25 dB higher than the previous device [11-12]. The low insertion loss and strong absorption and non-reciprocity confirms the low loss and strong magnon-phonon coupling of the fabricated device near the NV^- ground state transition frequency, holding great promise for the efficient and coherent excitation of ground state NV^- centers and the non-reciprocal quantum information transfer platforms.

References

- [1] Childress, L. & Hanson, R. Diamond NV centers for quantum computing and quantum networks. *MRS Bull.* **38**, 134–138 (2013).
- [2] Fuchs, G., Burkard, G., Klimov, P. & Awschalom, D. A quantum memory intrinsic to single nitrogen-vacancy centres in diamond. *Nat. Phys.* **7**, 789–793 (2011).
- [3] Taylor, J. et al. High-sensitivity diamond magnetometer with nanoscale resolution. *Nat. Phys.* **4**, 810–816 (2008).
- [4] de Lange, G., Riste, D., Dobrovitski, V. & Hanson, R. Single-spin magnetometry with multipulse sensing sequences. *Phys. Rev. Lett.* **106**, 080802 (2011).
- [5] Rondin, L. et al. Magnetometry with nitrogen-vacancy defects in diamond. *Rep. Prog. Phys.* **77**, 056503 (2014).
- [6] C. C. A. Teale, “Magnetometry with ensembles of nitrogen vacancy centers in bulk diamond,” thesis, Massachusetts Institute of Technology (2015).
- [7] H. Clevenson, M. E. Trusheim, C. Teale, T. Schroder, D. Braje, D. Englund, Broadband magnetometry and temperature sensing with a light-trapping diamond waveguide. *Nat. Phys.* **11**, 393–397 (2015).
- [8] A. Brenneis, L. Gaudreau, M. Seifert, H. Karl, M. S. Brandt, H. Huebl, J. A. Garrido, F. H. Koppens, A. W. Holleitner, Ultrafast electronic readout of diamond nitrogen-vacancy centres coupled to graphene. *Nat. Nanotechnol.* **10**, 135–139 (2015).
- [9] Labanowski, D. et al. Voltage-driven, local, and efficient excitation of nitrogen-vacancy centers in diamond. *Sci. Adv.* **4**, eaat6574 (2018).
- [10] Verba, R., Tiberkevich, V. & Slavin, A. Wide-Band Nonreciprocity of Surface Acoustic Waves Induced by Magnetoelastic Coupling with a Synthetic Antiferromagnet. *Phys Rev Appl* **12** (2019).
- [11] Shah, P. J. et al. Giant nonreciprocity of surface acoustic waves enabled by the magnetoelastic interaction. *Sci. Adv.* **6**, eabc5648 (2020).
- [12] Bas, D. A. et al. Nonreciprocity of phase accumulation and propagation losses of surface acoustic waves in hybrid magnetoelastic heterostructures. *Phys. Rev. Appl.* **18**, 044003 (2022).